

Ferroelectric and dielectric properties of strontium bismuth niobate vanadates

Yun Wu and Guozhong Cao^{a)}

Materials Science and Engineering, University of Washington, Seattle, Washington 98195

(Received 19 November 1999; accepted 20 April 2000)

Strontium bismuth niobate vanadates, $\text{SrBi}_2(\text{V}_x\text{Nb}_{1-x})_2\text{O}_9$ (with $0 \leq x \leq 0.1$), were prepared by reaction sintering of powder mixtures of constituent oxides. With partial substitution of niobium by vanadium cations (up to 10 at.%), the single-phase layered perovskite structure was preserved, and the sintering temperature of the system was significantly lowered (~ 200 °C). The incorporation of vanadium into the layered perovskite structure resulted in a shift of the Curie point to higher temperatures from 435 to 457 °C, with 10 at.% vanadium doping, and an increase in dielectric constant from ~ 700 to ~ 1100 , with 10 at.% vanadium doping, at their respective Curie points. The remanent polarization increased from ~ 2.4 to ~ 8 $\mu\text{C}/\text{cm}^2$, while the coercive field decreased from ~ 63 to ~ 45 kV/cm with 10 at.% V^{5+} doping.

I. INTRODUCTION

Ferroelectrics are excellent candidates for the applications in data storage in digital memory systems, in addition to many other important applications such as piezoelectrics, pyroelectrics, and electro-optics in sensors, actuators, and microelectromechanical systems (MEMS).^{1–5} Random-access memories (RAMs) based on semiconductor integrated technology have been a great success; however, these semiconductor RAMs can retain information only when power is on. A serious drawback is that when power is interrupted, all information is lost (volatile memory). Furthermore, these RAMs are very sensitive to radiation and this is detrimental for military and space applications.

Among ferroelectric materials, $\text{Pb}(\text{Zr,Ti})\text{O}_3$ (PZT) is one of the most popular materials attracting many investigators for many years. PZT has an isotropic perovskite crystal structure with a high remanent polarization ($30\text{--}50$ $\mu\text{C}/\text{cm}^2$).^{6–8} Unfortunately, PZT films tend to degrade most of the initial amount of switching charge (so-called “fatigue”) after $10^6\text{--}10^8$ cycles of full polarization switching.⁹ To be competitive with electrically erasable read-only memories (EEPROM), ferroelectric memories (FeRAMs), which are also called nonvolatile random-access memories (NvRAMs), must be improved to withstand at least 10^{12} erase/rewrite operations or they must have qualitatively different nondestructive read operations.³ Recently, bismuth oxide layered perovskite materials, such as $\text{SrBi}_2\text{Nb}_2\text{O}_9$ (SBN), $\text{SrBi}_2\text{Ta}_2\text{O}_9$

(SBT), and $\text{SrBi}_2(\text{Nb,Ta})_2\text{O}_9$ (SBTN), for FeRAM applications have attracted an increasing attention in the research community, because they are fatigue-free and lead-free and possess ferroelectric properties independent of film thickness.^{10,11} Layered perovskite ferroelectrics, however, suffer from two drawbacks: a relatively low remanent polarization and a high processing temperature.¹² Recently, efforts have been made to enhance the properties of layered perovskite ferroelectrics by the addition or substitution of alternative cations. For example, partial substitution of Sr^{2+} by Bi^{3+} has resulted in the most noticeable improvement of ferroelectric properties.^{13–15} Both the Curie point and the peak dielectric constant increased significantly with an increased Bi^{3+} substitution. The enhancement of ferroelectric properties was reported to be accompanied with a linear decrease in lattice parameters due to the substitution of relatively larger cations (Sr^{2+} : 143 pm) at A sites by relatively smaller cations (Bi^{3+} : ~ 130 pm). However, the substitution of bivalent Sr^{2+} cations by trivalent Bi^{3+} required introduction of cation vacancies to maintain electroneutrality. Although the influences of such cation vacancies on the ferroelectric properties have not been studied, cation vacancies may result in a structural distortion of oxygen octahedron and, thus, degrade the polarizability. The incorporation of barium ions into strontium positions was also reported to exhibit higher remanent polarization than the intrinsic $\text{SrBi}_2\text{Ta}_2\text{O}_9$ thin films.¹⁶

In our previous letters,^{17,18} we have reported that the significant enhancement of ferroelectric properties of SBN ferroelectrics through partial substitution of niobium by pentavalent vanadium cations. The enhanced ferroelectric properties were attributed to the increased rattling space inside the oxygen octahedron due to the

^{a)}Address all correspondence to the author.
e-mail: gzcao@u.washington.edu

smaller size of vanadium cations. In this paper, we will present a systematic study on the influences of vanadium doping on the dielectric and ferroelectric properties of SBN systems. The processing conditions, crystal and microstructures, and dielectric and ferroelectric properties of vanadium-doped SBN ferroelectrics were studied. In particular, the effects of vanadium doping on remanent polarization, coercive field, the Curie point, and direct current (dc) conductivity were discussed.

II. EXPERIMENTAL

The polycrystalline strontium bismuth vanadium niobate ceramic samples with a composition of $\text{SrBi}_2(\text{V}_x\text{Nb}_{1-x})_2\text{O}_9$ (SBVN) with x ranging from 0 to 0.1 (10 at.%) were prepared by solid-state reaction sintering. The starting materials used were SrCO_3 , Bi_2O_3 , V_2O_5 , and Nb_2O_5 (Aldrich Chem. Co., Milwaukee, WI), all with a purity of 99%. The powders were admixed with a desired weight ratio with approximately 4.5 wt% excess Bi_2O_3 , which was to compensate weight loss of Bi_2O_3 due to its high vapor pressure (750 mmHg at 1570 °C), which is on the order of that of lead oxide (750 mmHg at 1760 °C).¹⁹ Powders were ball milled with acetone for 24 h, and the mixtures were dried at 150 °C for 6 h. A two-step firing process was applied. The powder mixtures were first fired at 850–1000 °C in air for 2 h. The fired powders were ground and admixed with about 1–1.5 wt% poly(vinyl alcohol) (PVA; Aldrich Chem. Co.) as a binder and then pressed into pellets uniaxially at ~300 MPa. The pellets were then sintered in closed alumina crucibles at 950–1150 °C for 2 h in air. The typical firing conditions for samples with various compositions are summarized in Table I. Prior to characterization and property measurements, all the samples were annealed at 800 °C for 3 h in oxygen. X-ray diffractometry (XRD; Philips 1830, Eindhoven, The Netherlands), scanning electron microscopy (SEM; JEOL 52100, Tokyo, Japan), and optical microscopy were all used to characterize the fired powders and sintered pellets.

The pellets were polished to have flat and parallel surfaces and about 0.25–1 mm in thickness and electroded by sputtering Au/Pd or Pt on both sides for electrical property measurements. The dielectric constant and loss tangent as functions of temperature up to 600 °C and frequency ranging from 20 Hz to 1 MHz were measured

by a HP Precision LCR Meter 4284A (Hewlett Packard Co., Tokyo, Japan). The alternating current (ac) impedance data at various temperatures were also obtained using the HP 4284A LCR meter. The dc conductivity was estimated from the bulk resistance, R_g , which was derived from the equivalent circuit model in complex impedance planes of resistor and capacitor in parallel.²³

The P – E hysteresis loops were measured using a standard Sawyer–Tower circuit with a reference resistor of 10^7 ohm and a reference capacitor of 9.43×10^{-7} F. The parameters used for the measurement were the following: peak voltage, 3500 V; frequency, 10 Hz; wave form, triangle. Due to the high coercive field of the materials, the samples for the P – E hysteresis loop measurement were polished to ~0.25 mm in thickness. In addition, in order to get better P – E hysteresis loops, the measurements were conducted at temperatures of 165–178 °C, which are significantly lower than the Curie points.

III. RESULTS AND DISCUSSION

A. Sample preparation

XRD analyses (see Fig. 1) indicated that single-phase layered perovskites were formed within the composition range studied in this work; no secondary phase was detectable. Although pentavalent vanadium cations (58 pm) are much smaller in radius than that of pentavalent niobium cations (69 pm),²⁰ there was a slight decrease in crystal lattice constants as the amount of vanadium increased (see Table I). The change of crystal parameters was significantly smaller than that reported in the case of substitution of Sr^{2+} by Bi^{3+} .¹⁴

According to the work on isotropic perovskites, the structural stability could be described by the so-called “tolerance factor,” t , which is defined by²¹

$$R_A + R_O = t\sqrt{2(R_B + R_O)}, \quad (1)$$

where R_A , R_B , and R_O are the radii of respective A, B, and O ions in isotropic perovskite ABO_3 . A stable isotropic perovskite structure requires a tolerance factor between 0.80 and 1.02. The layered perovskite structure would be more restrictive, since the $(\text{Bi}_2\text{O}_2)^{2+}$ interlayers impose a great constraint for structural relaxation. Such a structural constraint induced from the $(\text{Bi}_2\text{O}_2)^{2+}$ interlayers may well explain the lack of an appreciable decrease in lattice parameters with an increased amount of vanadium

TABLE I. Compositions, sintering condition, relative density, and lattice parameters of the layered perovskite SBVN.

| Sample | Prefiring | Sintering condition | Relative density (%) | Lattice parameters (Å) ^a |
|---------------------|--------------|---------------------|----------------------|-------------------------------------|
| SBVN ($X = 0$) | 1000 °C, 2 h | 1150 °C, 0.5 h | 94 | $a = 3.900$, $c = 25.062$ |
| SBVN ($X = 0.05$) | 850 °C, 2 h | 950 °C, 2 h | 96 | $a = 3.898$, $c = 25.043$ |
| SBVN ($X = 0.1$) | 850 °C, 2 h | 950 °C, 2 h | 97 | $a = 3.897$, $c = 25.060$ |

^aThe accuracy of lattice parameters is 0.002 Å (pseudotetragonal).

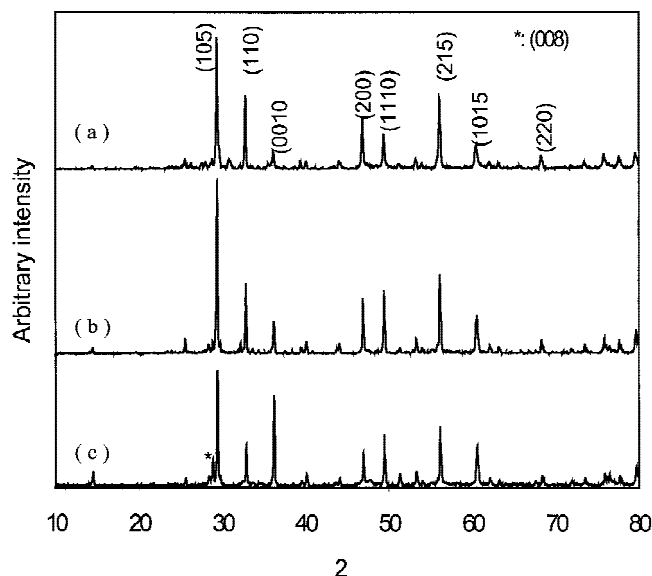


FIG. 1. XRD results of the SBVN pellets: (a) SBN pellet sintered at 1150 °C, 0.5 h; (b) SBN doped with 5% vanadium sintered at 950 °C, 2 h; and (c) SBN doped with 10% vanadium sintered at 950 °C, 2 h.

doping. This may further explain the fact that although the tolerance factor for $\text{SrBi}_2\text{V}_2\text{O}_9$ equals to 1.02, there exists no stable layered perovskite structure for this compound. The experimental results from this work indicated that although V^{5+} is too small to form a stable layered perovskite structure, the layered perovskite structure can be preserved with partial substitution by pentavalent vanadium cation, at least up to 10 at.%. The above results also imply that the vanadium doping SBN has a more “loose” crystal structure and there is a relatively larger space between the constituent ions, in particular, between the oxygen and vanadium ions.

A two-step firing process was applied in this study. The first step, firing at relatively low temperatures (850–1000 °C), was to promote the chemical reactions among the constituent compounds so as to form a single-phase layered perovskite. The second step, firing at relatively high temperatures (950–1150 °C), was to achieve high densification. Using this two-step firing process, all sintered pellets had a relative density above 94% (see Table I) and the total weight loss in all samples was found to be less than 3 wt% when the weight loss from the decomposition of SrCO_3 was excluded. This weight loss was presumably due to the evaporation of Bi_2O_3 and was less than the excess Bi_2O_3 that was initially added. Thus, all the samples presumably contained approximately 1.5 wt% excess Bi_2O_3 after sintering. The influences of the extra 1.5 wt% Bi_2O_3 on the physical properties would be the same in all the samples and, thus, is neglected hereinafter in discussing the influences of vanadium doping. SEM observation also revealed that there exists no detectable second phase and all samples

have a homogeneous microstructure. The incorporation of vanadium exhibits no appreciable influences on the microstructure of the layered perovskite, SBVN, ferroelectric ceramics.

Further, it was found that the addition of vanadium oxide lowered the sintered temperature at least 200 °C, while an appreciably higher density was achieved. In addition, the incorporation of vanadium appreciably improved the sinterability of ceramics (see Table I). The maximum achievable density for SBN sample was approximately 94%, while the samples with vanadium doping can easily reach a density of 96% or above. The lowered sintering temperature in this study is due partly to the low melting point of vanadium oxide (–690 °C), which was also reported as one effective sintering aid for low-firing ceramics,²² and also to the possible formation of an eutectic liquid phase in this multiple oxide system. Furthermore, it is noted that the sintering temperature used in the present study for the SBN is lower than that reported in the literature. For example, Chen *et al.*²³ prepared the SBN and SBT pellets by sintering the pellets at 1280 °C for 3 h. Torii *et al.*¹⁴ reported that SBT ceramic samples with relative density of 85–92% were prepared by sintering at 1200–1280 °C for 2 h in a closed alumina crucible.

B. *P*–*E* hysteresis loops

Figure 2 shows ferroelectric-characteristic temperature dependence of dielectric constant of three samples in the SBVN system at a frequency of 100 kHz with an oscillating amplitude (50 mV). The Curie point of the layered perovskites increased from 435 °C for SBN to 440 °C for SBVN with respective 5 at.% vanadium and 457 °C with 10 at.% vanadium doping. The peak dielectric constants at their respective Curie points also increased more than

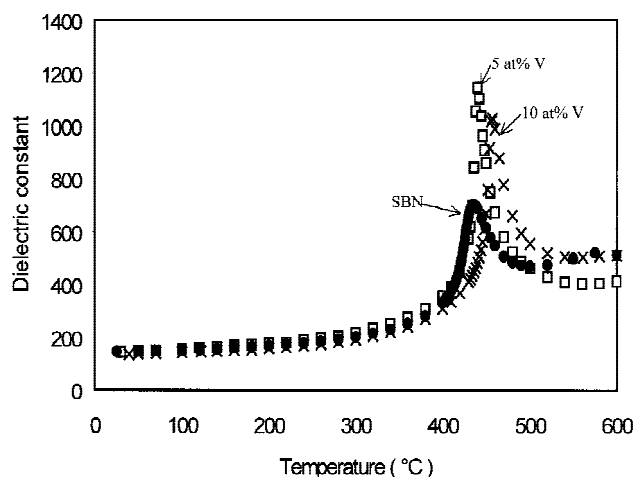


FIG. 2. Temperature dependence of dielectric constants of (●) SBN and (□) SBN with 5 at.% vanadium and (×) 10 at.% vanadium determined using a frequency of 100 kHz and an oscillation amplitude of 50 mV.

50%. Table II summarizes the Curie points and peak dielectric constants for all three samples. According to the literature on the layered perovskite ferroelectrics,²⁴ the shift of the Curie point to a higher temperature corresponding to a larger polarizability could well be explained by the increasing “rattling space” due to the incorporation of smaller pentavalent vanadium cations.²⁵ The shift of Curie point and the increase in peak dielectric constant corroborate the P - E hysteresis results described below.

Figure 3 shows the P - E hysteresis loops of the SBVN samples with $x = 0, 0.05$, and 0.1 , respectively. The P - E hysteresis loop of the SBN sample was measured at $178\text{ }^\circ\text{C}$, while those of SBVN with $x = 0.05$ and 0.1 were determined at $165\text{ }^\circ\text{C}$ with all other measurement parameters the same. This figure clearly demonstrated that the substitution of niobium by vanadium has a significant influence on the ferroelectric properties. The coercive field reduces from $2E_c = (E_{c+} - E_{c-}) = 125\text{ kV/cm}$ for SBN without vanadium doping to 80 – 90 kV/cm for SBVN with 5 – $10\text{ at.}\%$ vanadium doping. The remanent polarization increases significantly from approximately $2P_r = (P_{r+} - P_{r-}) = 4.8\text{ }\mu\text{C/cm}^2$ for SBN without vanadium doping to $2P_r = 7\text{ }\mu\text{C/cm}^2$ for $5\text{ at.}\%$ doped SBVN and to $2P_r = 16\text{ }\mu\text{C/cm}^2$ for $10\text{ at.}\%$ doped SBVN. For comparison, P_r and E_c for all three samples were also summarized in Table II. From the literature, typical $2P_r$ and $2E_c$ for SBN films were found to be around 5 – $20\text{ }\mu\text{C/cm}^2$ and 200 – 250 kV/cm .^{26–28} Considering the difference in measuring temperature and processing conditions, and the difference between thin films and bulk ceramics, the ferroelectric properties of the SBN ceramic in this study show very good agreement with the literature. It is also noted that no optimization of processing condition was conducted in this work. Better ferroelectric and dielectric properties would be obtained if the processing conditions were optimized.

The exact mechanism that the substitution of niobium by vanadium results in a significant enhancement of polarization and a decrease in coercive field is a subject for further study. One possible explanation is the increased “rattling space” inside the oxygen octahedron. The polarizability in isotropic perovskites (ABO_3) has been a subject of intensive study, and it has been found that the polarizability is largely determined by the sizes of A and B cations.²⁹ In general, a size decrease of B cations (lo-

cated inside an oxygen octahedron) results in an increase in both polarizability and the Curie point due to “a larger rattling space” available for B cations, provided that the perovskite structure is preserved. The size change of A cations has an opposite influence compared to that of B cations, since a size increase of A cations leads to an increased size of the oxygen octahedron and thus results in an increase in both polarizability and the Curie point. The crystal structure of SBN consists of the perovskite sheet ($\text{SrNb}_2\text{O}_7^{2-}$) interleaved with bismuth oxide layers where distorted NbO_6 octahedral are the origin of ferroelectricity as a result of the shift of Nb^{5+} away from the center position below the Curie temperature. Although V^{5+} can have 6 coordination of oxygen, it is too small to form a stable layered perovskite structure. However, partial substitution of Nb^{5+} by V^{5+} up to $10\text{ at.}\%$ results in a stable layered perovskite structure. A significant size decrease from Nb^{5+} (69 pm) to V^{5+} (58 pm), while without an appreciable decrease in crystal lattice constants (Table I), would certainly result in an increase in the rattling space inside the oxygen octahedron and thus a significant increase in polarization. In general, the substitution of alternative cations in isotropic perovskite ferroelectrics would have the effect of restricting domain wall motion and, thus, result in an increased coercive field.³⁰ A decrease in coercive fields with an increasing amount of vanadium substitution in the present study suggests a different mechanism being predominant. It is possible that vanadium cations with a much smaller ionic radius, resided inside almost unchanged oxygen octahedra, require a lower energy to rattle from one position to another inside the oxygen octahedron and thus lead to a lowered coercive field.

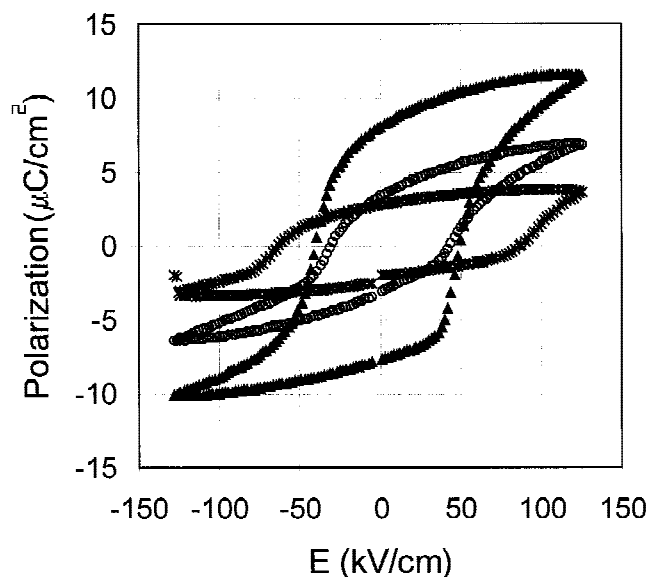


FIG. 3. P - E hysteresis loops for SBVN samples (*) at $178\text{ }^\circ\text{C}$ without vanadium, (O) at $165\text{ }^\circ\text{C}$ with $5\text{ at.}\%$ vanadium, and (▲) at $165\text{ }^\circ\text{C}$ with $10\text{ at.}\%$ vanadium.

TABLE II. Peak ϵ_r , E_c , and P_r of the layered perovskite SBVN samples.

| Sample | T_c ($^\circ\text{C}$) | Peak ϵ_r^a | E_c (kV/cm) | P_r ($\mu\text{C/cm}^2$) |
|---------------------|----------------------------|---------------------|---------------|------------------------------|
| SBVN ($X = 0$) | ~ 435 | ~ 700 | 63 | 3 |
| SBVN ($X = 0.05$) | ~ 440 | ~ 1140 | 40 | 3.5 |
| SBVN ($X = 0.1$) | ~ 456 | ~ 1040 | 50 | 8 |

^aMeasured with a frequency of 100 kHz .

The P - E hysteresis measurements were also performed at various temperatures for the vanadium-doped samples. Although the measuring temperatures are far below the Curie points, the samples showed higher spontaneous polarization at higher temperatures, which might be attributable to the expanded crystal lattice.

C. Frequency dependence

Figure 4 shows the dielectric constant and loss tangent as a function of frequency ranging from 20 Hz to 1 MHz at room temperature. There was a small variation in dielectric constants over the frequency range, while the loss tangent decreased noticeably from $\sim 4\%$ at 20 Hz to less than 1% at frequencies higher than 10^3 Hz. The samples with vanadium doping showed a slight decrease in dielectric constants at room temperature, particularly at a high substitution content (10 at.%), while vanadium doping (noticeably 5 at.%) resulted in only a negligible increase in loss tangent at frequencies below 10^3 Hz.

Dielectric constant, ϵ_r , is a combined contribution of four polarization: atomic polarization (ϵ_a , responding frequency, 10^{15} Hz); ionic polarization (ϵ_i , 10^{13} Hz); dipolar polarization (ϵ_d , $\sim 10^{10}$ Hz); space charge (ϵ_s , $\sim 10^2$ Hz).³⁰

$$\epsilon_r = \epsilon_a + \epsilon_i + \epsilon_d + \epsilon_s \quad (2)$$

At frequencies below $\sim 10^2$ Hz, all polarization mechanisms, including space charge, contribute to dielectric constant; however, at frequencies above 10^2 Hz, space charge will no longer contribute to the dielectric constant. A negligible change of dielectric constant as frequency changes from low frequencies to high frequencies (above 10^3 Hz) implies that there is no appreciable contribution of space charge.

The experimental results obtained above, (i.e., constant ϵ_r over a wide frequency range), imply that the incorporation of vanadium cations into the layered

perovskite structure did not lead to a significant increase in space charge. This further indicates that the incorporation of vanadium into the crystal structure did not introduce mobile charge carriers: free electrons, electron holes, or oxygen vacancies. This observation could be explained by two possible mechanisms. One is that pentavalent vanadium cations are stable in the layered perovskite structure, particularly after oxygen annealing and, thus, no oxygen vacancies are created and no oxygen ionic conduction is introduced to the system. Another possibility is that there might coexist both tetra- and pentavalent vanadium cations; however, the multivalent and variable valent vanadium cations did not form continuous chains which are required for the nearest neighbor hopping conduction mechanism. In the latter, there would exist oxygen vacancies so as to satisfy the electroneutrality. As discussed above, these oxygen vacancies would contribute to ionic conduction and lead to space charge polarization. The lack of space charge polarization in the vanadium-doped layered perovskite system indicates that it is unlikely that there exists tetravalent vanadium cations. However, it is possible that if the vanadium doping content exceeds a critical point, a hopping chain may form, resulting in an appreciable increase in both loss tangent and electrical conductivity. For example, in the $\text{Bi}_2\text{VO}_{5.5}$ system, with niobium substitution for vanadium ($\text{Bi}_2\text{Nb}_x\text{V}_{1-x}\text{O}_{5.5}$), both the dielectric constant and the loss tangent value decrease with a decreased amount of vanadium.³¹ However, it is worthy to notice that a reduction of loss tangent as frequency reduces from 20 to 10^3 Hz (see Fig. 4) implies that there exists structural relaxation at low frequencies.

Figure 5 shows the loss tangent at 100 kHz from room temperature to 600 °C. The tangent losses of all three samples increase as the temperature rises. However, the values were very similar and rather low at temperatures

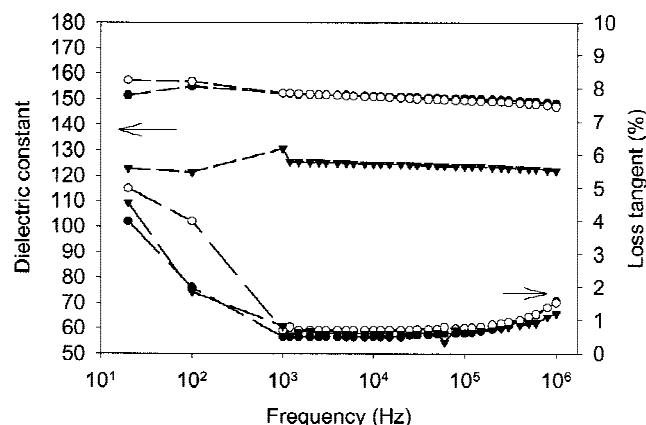


FIG. 4. Dielectric constants and tangent loss of the three samples over frequency at room temperature: (●) SBN sample, (○) SBN doped with 5% vanadium, and (▼) SBN doped with 10% vanadium.

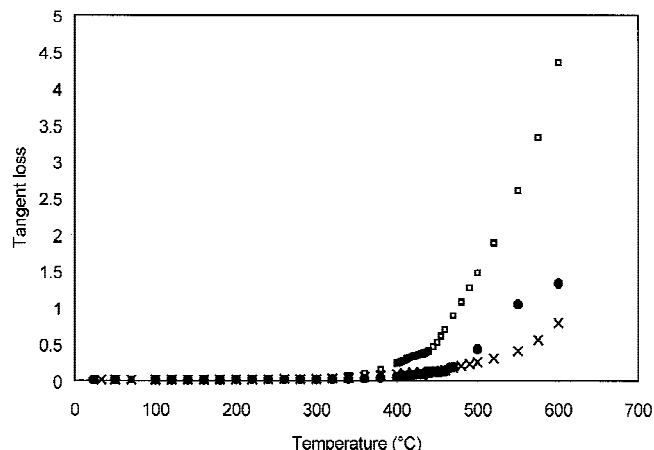


FIG. 5. Temperature dependence of dielectric loss at 100 kHz for (□) SBN sample and (●) SBN doped with 5 at.% vanadium and (×) 10 at.% vanadium.

below 400 °C. Above 400 °C (near their Curie points) the loss tangents increase rather quickly. Among them, the sample without vanadium doping shows much higher tangent loss values and the sample with the highest amount of vanadium doping (10 at.%) shows the lowest loss values. This suggests that, at the high frequency range (around 100 kHz) at temperatures near the Curie point, the dielectric losses at high temperature were minimized by the partial doping of vanadium. It is not known if it could be attributed to the structural complication due to the vanadium doping.

D. Electrical conduction

The dc conductivity of new layered perovskite ferroelectrics, SBVN, was studied by means of the ac impedance measurements at temperatures ranging from 60 to 700 °C in a frequency range from 20 Hz to 1 MHz. This dc conductivity was estimated from the bulk resistance, R_g , which was derived from the equivalent circuit model in complex impedance planes of resistor and capacitor in parallel.²³ Figure 6 shows the bulk ionic conductivity of the SBVN ferroelectrics as a function of temperature. For all three cases, a transition temperature between 250 and 320 °C was observed at which the conduction mechanism changed. There are two predominant conduction mechanisms at different temperature ranges, regardless of vanadium doping. At temperatures below the transition point, the electrical conduction is likely dominated by extrinsic defects, such as unintentionally introduced impurities, and the dc conductivity for all three samples was found the same of approximately 2×10^{-9} S/cm. This dc conductivity is approximately 2 orders of magnitude lower than that reported in literature²³ but still higher than the result from PZT.³² At temperatures higher than the transition point, the conduction is presumably dominated by the intrinsic defects. It is found

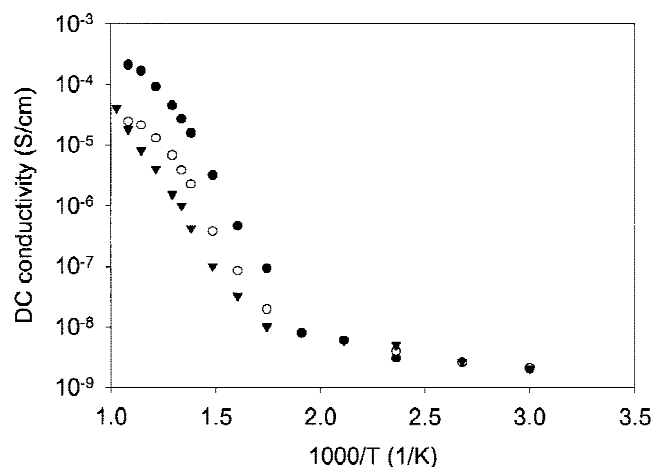


FIG. 6. Temperature dependence of dc conductivity of (●) pure SBN sample and (○) SBN doped with 5 at.% vanadium and (▼) 10 at.% vanadium.

that the dc conductivity of the SBVN ceramics decreased with an increased doping content at the higher temperature range, while there was an appreciable decrease in activation energy from 1.174 to 1.074 eV as the vanadium doping increased from 0 to 10 at.%. Table III summarizes the conduction transition temperature, activation energies for intrinsic conduction, and dc conductivity at 60 °C.

For a single-phase material with a homogenous microstructure, the electrical conductivity, σ , depends on both the concentration and mobility of charge carriers and can be presented by the following simplified equation:

$$\sigma = nq\mu = A \exp(-E_a/kT) \quad , \quad (3)$$

where n is the concentration of charge carriers, q the number of charges per charge carrier, μ the mobility of charge carriers, A a temperature-independent constant, E_a the nominal activation energy per charge carrier, k Boltzman's constant, and T the temperature. At low temperatures, when the extrinsic conduction is predominant, the nominal activation energy equals diffusion activation energy. However, at high temperatures when intrinsic conduction predominates, the nominal activation is the sum of diffusion activation, E_d , and formation energy of charge carrier, E_f :

$$E_a = E_d + E_f \quad . \quad (4)$$

Therefore, a reduced dc conductivity suggests a reduced concentration and/or mobility of charge carriers. The substitution of niobium by vanadium may result in increased complexity in the crystal structure and, thus, a reduced mobility (or diffusivity) of charge carriers. A decrease in activation energy with an increasing amount of vanadium doping, however, suggests that the concentration of intrinsic charge carriers may increase due to the incorporation of vanadium cations. If the primary intrinsic charge carriers in the layered perovskite ferroelectrics, SBVN, are oxygen vacancies, a relatively lower diatomic bond strength of V–O bonds (~ 627 kJ/mol), as compared to that of Nb–O bonds (~ 703 kJ/mol),¹⁹ could be responsible for the reduced activation energy with an increasing amount of vanadium doping. In addition, the multivalence state of vanadium cations may contribute extra electrical conduction, leading to a lower activation energy. The experimental results observed in this study

TABLE III. Activation energies, transition temperature, and bulk ionic conductivity at 60 °C for SBVN ferroelectrics.

| Sample | E_a (eV) | T_{Trans} (°C) | σ_{dc} at 60 °C (S/cm) |
|---------------------|------------|-------------------------|--------------------------------------|
| SBVN ($X = 0$) | 1.174 | ~ 250 | 2.12×10^{-9} |
| SBVN ($X = 0.05$) | 1.114 | ~ 280 | 2.14×10^{-9} |
| SBVN ($X = 0.1$) | 1.074 | ~ 320 | 2.09×10^{-9} |

suggest that the effects of vanadium doping on the dc conduction is complex, and further analysis is required to achieve a better understanding.

The above discussion was based on the assumption that the microstructure of all SBVN samples remains the same regardless of the vanadium substitution. It is assumed that all vanadium was incorporated into layered perovskite structure and no grain boundary phase or secondary phase was formed. Our XRD and SEM observation supported the above assumption. However, XRD and SEM may not be sensitive enough to reveal the fine details of microstructure due to their relatively low sensitivity and/or magnification. More detailed microstructure analysis, e.g., transmission electron microscopy, is needed to verify the above assumption.

Figure 7 is the ac conductivity at 100 kHz of these samples. The abnormal conductivity was observed at their Curie points for all the samples which might be influenced by the corresponding phase transitions. After this conductivity peak, the conductivity of SBN increases much faster than the doped samples. This might be due to the same mechanisms we discussed in the bulk ionic conductivity measurements.

IV. SUMMARY

In summary, the dielectric and ferroelectric properties of the layered perovskite, SBN, have been significantly enhanced with vanadium doping up to 10 at.%, while the layered perovskite structure was preserved. Substitution of niobium by much smaller vanadium cations, while without an appreciable decrease in crystal lattice constants, resulted in an increased rattling space for the cations inside the oxygen octahedra, leading to a higher Curie temperature and a larger dielectric constant at the Curie point. In addition, the increased rattling space

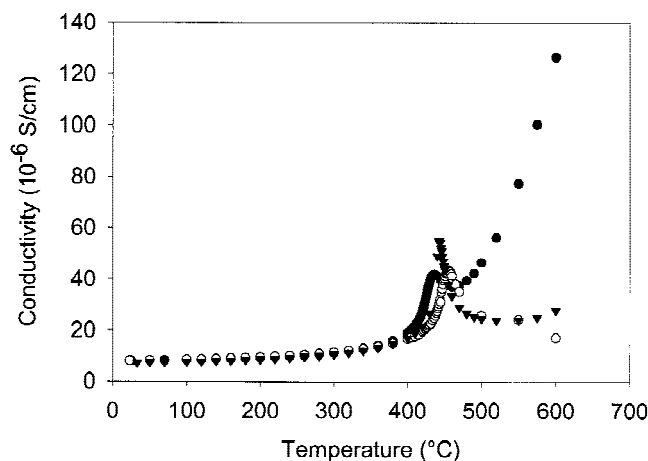


FIG. 7. Temperature dependence of ac conductivity of (●) pure SBN sample and (○) SBN doped with 5 at.% vanadium and (▼) 10 at.% vanadium at 100 kHz.

resulted in a significantly higher remanent polarization from ~ 2.4 to $\sim 8 \mu\text{C}/\text{cm}^2$ and lower coercive field from ~ 63 to $\sim 45 \text{ kV}/\text{cm}$ with 10 at.% V^{5+} doping. Furthermore, experiments revealed that the incorporation of vanadium did not increase the loss tangent and the dc conductivity. On the contrary, the loss tangent at 100 kHz decreased by the vanadium doping at temperatures near the Curie point. At lower temperatures, the SBVN samples show almost the same ac ($\sim 10^{-6} \text{ S}/\text{cm}$ at 100 kHz) and dc conductivity ($\sim 10^{-9} \text{ S}/\text{cm}$) regardless vanadium doping, while, at the higher temperature range ($>320^\circ\text{C}$), the vanadium-doped samples showed lower dc conductivity. Reduced dc conductivity at high temperatures may be attributed to the increased complexity in crystal structure and, thus, a reduced mobility of charged carriers, with partial substitution of niobium by vanadium.

ACKNOWLEDGMENTS

The authors thank Dr. Chen Ang and Dr. Zhi Yu for the P - E hysteresis measurements. Dave Rice and Scott Bulkley are acknowledged for general technical support. Partial financial support from the Center for Nanotechnology is gratefully acknowledged.

REFERENCES

1. M.E. Lines and A.M. Glass, *Principles and Applications of Ferroelectrics and Related Materials* (Clarendon Press, Oxford, United Kingdom, 1977).
2. *Ferroelectric Thin Films VI*, edited by R.E. Treece, R.E. Jones, C.M. Foster, S.B. Desu, and I.K. Yoo (Mater. Res. Soc. Symp. Proc. **493**, Warrendale, PA, 1998).
3. J.F. Scott and C.A. de Araujo, *Science* **246**, 1400 (1989).
4. R.E. Jones, Jr., P.D. Maniar, R. Moazzami, P. Zurcher, J.Z. Witowski, Y.T. Lii, P. Chu, and S.J. Gillespie, *Thin Solid Films* **270**, 584 (1995).
5. G.Z. Cao, in *Advances in Materials Science & Applications*, edited by D.L. Shi (Tsinghua University Press, Beijing, China, in press).
6. C.H. Ahn, R.H. Hammond, T.H. Geballe, M.R. Beasley, J.M. Triscone, M. Decroux, O. Fischer, L. Antognazza, and K. Char, *Appl. Phys. Lett.* **70**, 206 (1997).
7. B.A. Tuttle, in *Thin Film Ferroelectric Materials and Devices*, edited by R. Ramesh (Kluwer, Norwell, MA, 1998), p. 145.
8. M. Shimizu, H. Fujisawa, and T. Shiosaki, *Microelectron. Eng.* **29**, 173 (1995).
9. H. Watanabe, T. Mihara, H. Yoshimori, and C.A. Paz de Araujo, *Jpn. J. Appl. Phys.* **34**, 5240 (1995).
10. J.F. Scott, F.M. Ross, C.A. Paz de Araujo, M.C. Scott, and M. Huffman, *Mater. Res. Bull.* **21**, 33 (1996).
11. C.A. de Araujo, J.D. Cuchlaro, L.D. McMillan, M.C. Scott, and J.F. Scott, *Nature* **374**, 627 (1995).
12. J.F. Scott, in *Thin Film Ferroelectric Materials and Devices*, edited by R. Ramesh (Kluwer, Norwell, MA, 1997), p. 115.
13. P. Duran-Martin, A. Castro, P. Millan, and B. Jimenez, *J. Mater. Res.* **13**, 2565 (1998).
14. Y. Torii, K. Tato, A. Tsuzuki, H.J. Hwang, and S.K. Dey, *J. Mater. Sci. Lett.* **17**, 827 (1998).

15. H. Watanabe, T. Mihara, H. Yoshimori, and C.A.P. Araujo, *Jpn. J. Appl. Phys.* **34**, 5240 (1995).
16. C. Lu and C. Wen, in *Ferroelectric Thin Films VII*, edited by R.E. Jones, R.W. Schwartz, S.R. Summerfelt, and I.K. Yoo (Mater. Res. Soc. Symp. Proc. **541**, Warrendale, PA, 1999), p. 229.
17. Y. Wu and G.Z. Cao, *Appl. Phys. Lett.* **75**, 2650 (1999).
18. Y. Wu and G.Z. Cao, *J. Mater. Sci. Lett.* **19**, 267 (2000).
19. *CRC Handbook of Chemistry and Physics*, 61st ed., edited by R.C. Weast and M.J. Astle (CRC Press, Boca Raton, FL, 1974).
20. R.D. Shannon and C.T. Prewitt, *Acta Crystallogr. B* **25**, 925 (1969).
21. V.A. Isupov, *Inorg. Mater.* **33**, 936 (1997).
22. S. Cho, H. Yoon, D. Kim, T. Kim, and K. Hong, *J. Am. Ceram. Soc.* **81**, 3038 (1998).
23. T. Chen, C. Thio, and S.B. Desu, *J. Mater. Res.* **12**, 2628 (1997).
24. K. Singh, D.K. Bopardik, and D.V. Atkare, *Ferroelectrics* **82**, 55 (1988).
25. E.C. Subbarao, *Integr. Ferroelectr.* **12**, 33 (1996).
26. K. Kato, C. Zheng, J.M. Finder, and S.K. Dey, *J. Am. Ceram. Soc.* **81**, 1869 (1998).
27. S.B. Desu and D.P. Vijay, *Mater. Sci. Eng. B* **32**, 83 (1995).
28. S.B. Desu and T. Li, *Mater. Sci. Eng. B* **34**, L4 (1995).
29. F. Jona and G. Shirane, *Ferroelectric Crystals* (Pergamon Press, New York, 1962).
30. A.J. Moulson and J.M. Herbert, *Electroceramics: Materials, Properties, Applications* (Chapman & Hall, London, United Kingdom, 1990).
31. K.B.R. Varma and K.V.R. Prasad, *J. Mater. Res.* **11**, 2288 (1996).
32. Y. Lee, L. Wu, C. Liang, and T. Wu, *Ferroelectrics* **138**, 11 (1993).